Environmental Health Perspectives
Vol. 54, pp. 135–145, 1984

NMR Analysis of the Structure and Metal Sequestering Properties of Metallothioneins

by Catherine T. Hunt,* Yvan Boulanger,† Stephen W. Fesik‡ and Ian M. Armitage*

^{113}Cd–NMR studies have been used to elucidate the structure of the metal–binding sites in mammalian and invertebrate (*Scylla serrata*) metallothioneins (MTs). Chemical shift data have shown that all Cd ions are tetrahedrally coordinated to four cysteine thiolate ligands with single cysteinyl sulfurs bridging adjacent metals. Homonuclear decoupling experiments have shown that the 7 g–atoms of metal bound per mole of mammalian protein are located in a three– and a four–metal cluster while the 6 g–atoms of metal in the invertebrate MT are located in two three–metal clusters. The different metal binding affinities of the two mammalian clusters have been determined by ^{113}Cd–NMR. The three–metal cluster prefers Cu > Zn > Cd whereas exactly the reverse order applies in the four–metal cluster. Proteolytic cleavage of the protein produced a 32–residue fragment which contained the four–metal cluster and demonstrated the presence of two separate domains in the protein. 500 MHz ^{1}H–NMR has been employed to elucidate the arrangement of these metal clusters in the tertiary structure of the protein. The ^{1}H resonances were assigned from their scalar and dipolar connectivities obtained from extensive one and two–dimensional NMR experiments. A specific application of 2D correlation spectroscopy (COSY) to the assignment of the ^{1}H resonances in crab MT–1 is discussed. A molecular model, representing the three–dimensional solution structure of this protein, has been constructed based on an analysis of all these data. Detailed structural features of this model are discussed, with particular emphasis on their relationship to the function and evolution of the protein.

Introduction

Metallothioneins (MTs) are a class of low molecular weight (~6100 dalton), cysteine-rich, metal-binding proteins found ubiquitously in nature (*1–4*). The protein is known to bind various metal ions such as cadmium, zinc, copper and mercury (*5*), and its biosynthesis is closely regulated by the level of exposure of an organism to salts of these metals (*6 – 8*). For these reasons it is quite widely accepted that MTs function as detoxifying agents by sequestering toxic metals (*9*), but it has also been suggested that MTs function in the regulation and/or metabolism of essential heavy metals (*10,11*).

Shortly after the discovery (*12*) and sequencing of metallothionein from horse kidney cortex (*13,14*), it was found that 20 of the 61 amino acid residues of mammalian MTs are cysteines, all of which participate in the ligation of 7 g-atoms of metal (*5*). Subsequent studies revealed that a remarkable homology exists in the amino acid sequences of all mammalian MTs (*2,13–18*). In fact, the positions of all the 20 cysteine residues are invarient along with those of 18 other residues. This suggests that specific metal–thiolate interactions are important for the structural and functional viability of the protein. This will be discussed in light of the fact that MTs from non-mammalian sources possess shorter amino acid chains with a smaller number of cysteines (Fig. 1) and bind fewer metals. MT generally exists in two isoprotein forms, MT-1 and MT-2, which differ in amino acid composition and total charge (*19*). Structural characterization of this protein has been slow because of its elusive properties such

*The Department of Molecular Biophysics and Biochemistry, Yale University, New Haven, CT 06510.
†Present affiliation: Institut de Génie Biomédical, Université de Montréal, C.P. 6128, Succ. A, Montreal, Quebec, Canada H3C 3J7.
‡Present affiliation: Abbott Laboratories, D–47F, Abbott Park, North Chicago, IL 60064

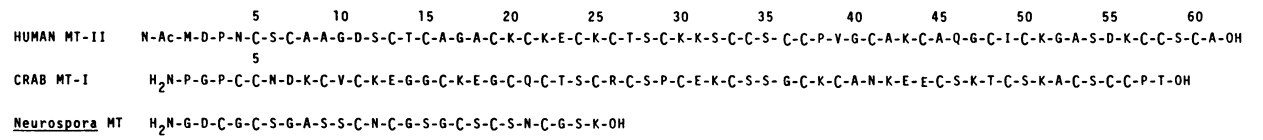

FIGURE 1. Amino acid sequence of metallothionein from different sources.

as, the large number of repetitive residues (Cys, Lys, Ser) and the lack of both aromatic residues and histidine (*19*). Previously reported UV and CD data (*5,20–23*) are indicative of metal–sulfur ligation but assertions of tetrahedral coordination (*23*) based on these data must be viewed with caution because of the severe overlap of the metal–thiolate charge transfer bands. The metal ions commonly found in MTs—Cu^+ (*24*), Zn^{2+} and Cd^{2+}—are all diamagnetic and therefore unsuitable for ESR studies.

In view of these factors, ^{113}Cd–NMR has become a key in the study of the structure of the metal-binding sites in metallothionein. The tremendous sensitivity of ^{113}Cd chemical shifts to subtle differences in metal environments (*25*) has made it possible to observe a separate ^{113}Cd resonance for each of the metal ions in the protein, in spite of their similar coordination sites (*26*). Analysis of ^{113}Cd-NMR data from rabbit (*27*), human (*28*), calf (*29*) and crab (*30,31*) MTs provided the first direct evidence for the arrangement of these metals in two separate polynuclear clusters. For mammalian MTs, the 7 g-atoms of metal are present in a three- and a four-metal cluster, while in an invertebrate MT the 6 g-atoms of metal are present in two three-metal clusters (*27,32*). These and further studies have shown that the two clusters in mammalian MTs exhibit significant differences in their affinities for different metal ions and that they function quite independently of one another (*28–30,33*).

In order to further extend our knowledge of the secondary and tertiary structure of the protein, Chou-Fasman calculations and 500 MHz ^1H-NMR studies have been employed (*34*). Scalar and dipolar connectivities between the protons of several different residues were obtained from extensive one- and two-dimensional NMR experiments. Based on an analysis of these and previously summarized physicochemical data (*34*), a molecular model representing the three-dimensional solution structure of this protein has been constructed. Detailed structural features of this model will be discussed with particular emphasis on the existence of two independent domains and their relationship to the function and evolution of this protein.

^{113}Cd-NMR of Invertebrate Metallothionein

Metallothionein from mud crab (*Scylla serrata*) hepatopancreas binds 6 g-atoms of metal per mole of protein and contains 58 (MT-1) or 57 (MT-2) amino acids, 18 of which are cysteines (*35*). This invertebrate MT, like the mammalian MTs, can be induced by the administration of cadmium (*36*). Native crab MT isolated from ^{113}Cd-injected crabs is homogeneous in its metal composition (*36,37*) and is therefore particularly amenable to study by ^{113}Cd-NMR (*31*). Figure *2A* shows the ^1H-decoupled ^{113}Cd-NMR spectrum of native crab ^{113}Cd-MT-1. The chemical shifts of the ^{113}Cd resonances (between 620 and 660 ppm) are consistent with coordination to four cysteinyl sulfurs (*38,39*). The six separate ^{113}Cd resonances (3 and 4 overlap slightly) correspond to the individual metal binding sites. The multiplet structure of each of the resonances is due to ^{113}Cd–^{113}Cd scalar coupling and has provided evidence that all six $^{113}Cd^{2+}$ ions are located in polynuclear metal clusters (*25–27,32*). The structure of these clusters was determined by homonuclear decoupling experiments (*30*), two of which are shown in Figures 2*B* and 2*C*. In Figure 2*B*, selective irradiation of resonance 1 resulted in the collapse of resonances 2 and 6, while irradiating the overlapping resonances 3 and 4 in Figure 2*C* collapsed resonance 5 to a singlet. It was therefore concluded that the metals are located in two three-metal clusters, one containing the $^{113}Cd^{2+}$ ions giving rise to resonances 1, 2 and 6 and the other containing the metals corresponding to resonances 3, 4 and 5. The magnitude of the observed ^{113}Cd–^{113}Cd spin coupling (19–43 Hz) is suggestive of a two-bond interaction (*31*), presumably via a bridging thiolate ligand. From these data, it is possible to propose a structure for the three-metal cluster in which each cluster forms a six-membered ring consisting of three sulfur and three cadmium atoms (Fig. 3, cluster B). Each Cd^{2+} is tetrahedrally coordinated to four cysteines, and thus nine cysteines are involved in the formation of each cluster, $Cd_3(Cys)_9$. This structure for the two three-metal clusters in crab MT is therefore consistent with the participation of all 18 cysteines

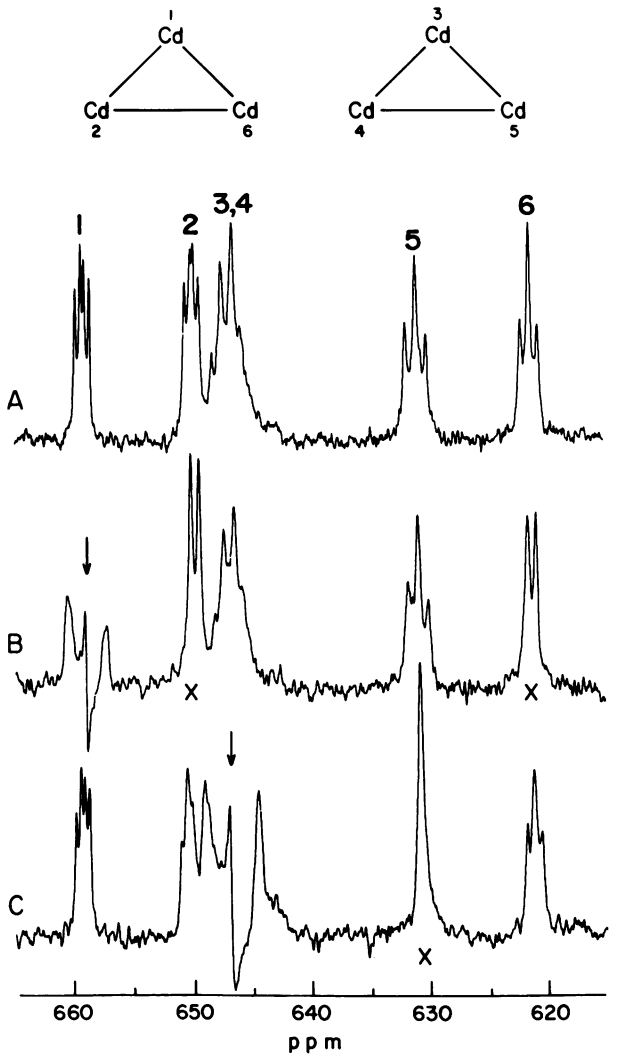

FIGURE 2. ^{113}Cd-NMR spectra at 44.4 MHz of native crab MT-1 (~8 mM; Cd:Zn = 60:1) in 0.01 M Tris, 0.1 M NaCl, pH 9.0: (*A*) proton decoupled spectrum (23,000 transients); (*B,C*) same as *A* but with homonuclear decoupling pulses applied at the frequencies indicated by an arrow and the affected resonances designated by X (*31*).

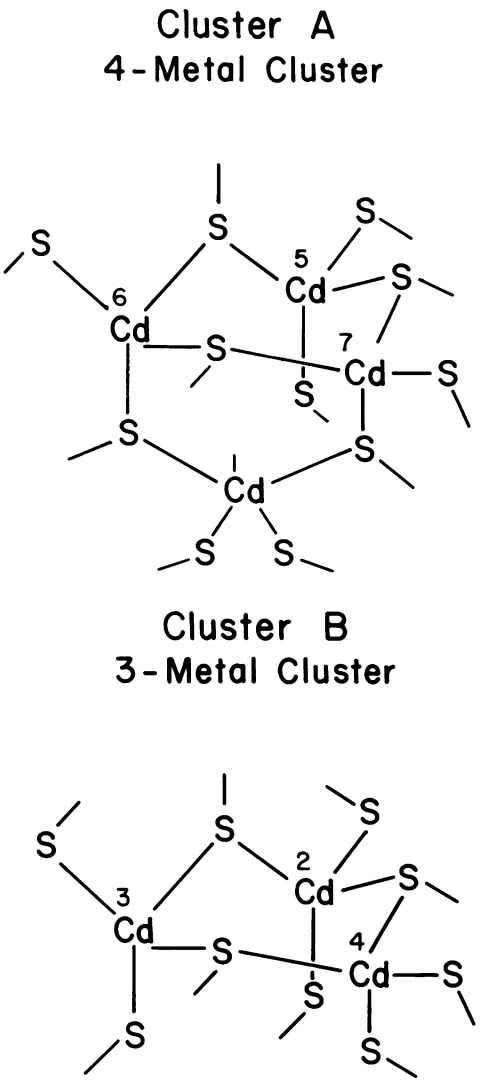

FIGURE 3. Proposed structures of the four-metal and three-metal clusters of mammalian metallothioneins based on ^{113}Cd-NMR data. The Cd numbering corresponds to the chemical shifts of the ^{113}Cd-NMR multiplets (Fig. 4) (27).

in metal binding. In the other isoprotein of crab metallothionein, MT-2, the ^{113}Cd chemical shifts are slightly different as a result of the different amino acid composition but the results of the homonuclear decoupling experiments again demonstrate the presence of two three-metal clusters.

^{113}Cd-NMR of Mammalian Metallothioneins

Mammalian MTs bind 7 g-atoms of metal per mole of protein and contain 61 amino acids, 20 being sequence invarient cysteine residues (*13–19*). The positions of 18 other residues, mostly lysine and serine, are also invarient. This suggests that their positions are important to the physiological function of the protein. The individual metal coordination sites of rabbit (*27*), human (*28*) and calf (*29*) liver metallothioneins have been elucidated by ^{113}Cd-NMR experiments similar to those used in the study of native ^{113}Cd-induced crab MT. While native crab ^{113}Cd-MT was found to be homogeneous in metal content, this was not the case for the ^{113}Cd-induced mammalian MTs studied. The cadmium-induced rabbit MTs contained, in addition to Cd^{2+}, a substantial

amount of Zn^{2+} which was not randomly distributed among the multiple metal binding sites (*32*). This heterogeneity in metal composition resulted in a ^{113}Cd-NMR spectrum of native rabbit ^{113}Cd,Zn-MT which was complicated due to the sensitivity of the ^{113}Cd chemical shifts to the presence of Zn^{2+} at neighboring sites in the clusters.

In order to facilitate the assignment of the ^{113}Cd spectrum, all of the Zn^{2+} ions in several rabbit MT preparations were replaced with $^{113}Cd^{2+}$ by adding cadmium salts directly to the tissue homogenate during extraction (*27*). The ^{113}Cd-NMR spectrum of reconstituted rabbit ^{113}Cd-MT-1 is shown in Figure 4*A* and is considerably simpler than that of the native rabbit MT (*27*). The chemical shifts of the ^{113}Cd resonances (610–670 ppm) span a slightly larger range than those of crab MT (Figs. 4*A* and 4*D*) but are entirely consistent with coordination to four cysteinyl sulfurs. Selective homonuclear decoupling experiments on reconstituted rabbit ^{113}Cd-MT identified the presence of two separate polynuclear metal clusters. There is a three-metal cluster corresponding to the $^{113}Cd^{2+}$ ions giving rise to resonances 2, 3 and 4 and a four-metal cluster corresponding to the $^{113}Cd^{2+}$ ions giving rise to resonances 1, 5, 6 and 7. Duplication in the resonances from the four-metal cluster (1′, 5′, 6′ and 7′) presumably stems from the sensitivity of the ^{113}Cd chemical shifts to heterogeneity in the primary structure of the MT (*25*). That is, each of the major isoproteins (MT-1 and MT-2) from rabbit liver is a mixture of at least two proteins.

The ^{113}Cd-NMR spectrum of reconstituted human ^{113}Cd-MT-1, which is homogeneous in metal composition, is remarkably similar to that of rabbit as seen by comparing spectra *A* and *B* in Figure 4. Complete analysis confirmed that human Cd–MT contains the same two-cluster arrangement (*28*). There was no duplication of ^{113}Cd resonances for human MT-2 because there is no heterogeneity in its primary sequence. Human MT-1, however, shows duplication in resonance 4 of the three-metal cluster and resonance 5 of the four-metal cluster. This is consistent with the fact that human MT-1 is a mixture of at least three proteins (*40*) with sequence heterogeneity at six positions (*18*).

Even after reconstitution with $^{113}Cd^{2+}$ in a manner similar to that used for rabbit and human MTs, calf liver MT was heterogeneous in metals, containing both Cu^{+} and Cd^{2+} in a ratio of approximately 3 to 4 (*29*). However, unlike the hybrid rabbit ^{113}Cd,Zn-MT, the hybrid calf ^{113}Cd,Cu-MT exhibited a remarkably simple spectrum as shown in Figure 4*C*. There were only four major resonances, and these displayed chemical shifts in positions already assigned to the four-metal cluster of human and rabbit MT. This was confirmed by homonuclear decoupling experiments. The lack of ^{113}Cd resonances corresponding to the three-metal cluster (between 635 and 665 ppm) indicated that it was occupied by Cu^{+}. The different metal affinities of the two clusters will be discussed in a subsequent section.

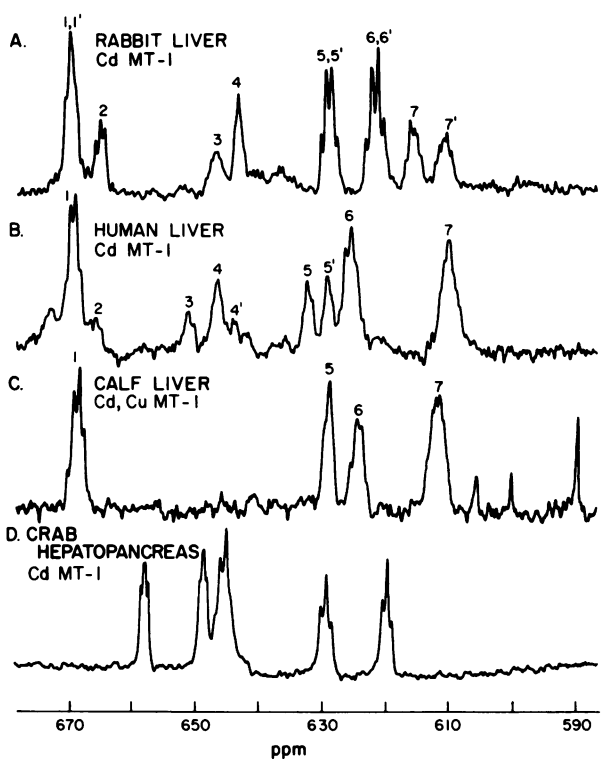

FIGURE 4. Comparison of the proton-decoupled ^{113}Cd-NMR spectra at 44.4 MHz of ^{113}Cd reconstituted mammalian metallothioneins and ^{113}Cd-induced invertebrate metallothionein: (*A*) rabbit liver Cd-MT-1 (~ 8 mM; Cd:Zn = 40:1); (*B*) human liver Cd-MT-1 (~7 mM; Cd:Zn = 50:1); (*C*) calf liver Cd,Cu-MT-1 (~6 mM; Cd:Cu = 1.45:1); (*D*) *Scylla serrata* hepatopancreas Cd-MT-1 (~8 mM; Cd:Zn = 60:1).

In order to be consistent with these data and in order to utilize all 20 cysteines in metal ligation, the structures shown in Figure 3 have been proposed for the two separate clusters in mammalian MTs. The three-metal cluster forms a cyclohexane-like six-membered ring requiring nine cysteine thiolate ligands, $Cd_3(Cys)_9$, as seen in crab MT. The four-metal cluster forms a bicyclo[3:1:3] structure requiring the remaining 11 cysteine thiolate ligands, $Cd_4(Cys)_{11}$. This results in two types of metal coordination. Two metals (labeled 6 and 7) are coordinated by three bridging sulfur

ligands and one nonbridging sulfur, and these give rise to the most shielded resonances in the spectrum. The other five metals are each liganded to two bridging and two nonbridging thiolates and give rise to more deshielded resonances (Figs. 4*A* and 4*B*).

Metal-Binding Affinity

The ^{113}Cd-NMR studies summarized above have provided considerable insight into the relative affinities of the two mammalian metal clusters for different metal ions. The ^{113}Cd-NMR study of calf liver ^{113}Cd,Cu-MT has shown that the $^{113}Cd^{2+}$ ions are bound to the four-metal cluster, whereas the ESR-silent Cu^+ ions are located in the three-metal cluster (*29*). Thus, the four-metal cluster exhibits a preference for Cd^{2+} over Cu^+, while the opposite is true for the three-metal cluster. Furthermore, since reconstituted calf liver ^{113}Cd,Cu-MT was prepared by *in vitro* replacement of Zn^{2+} by $^{113}Cd^{2+}$ in native Zn,Cu-MT (*29*), one can conclude that the native protein contained Zn^{2+} in the four-metal cluster and Cu^+ in the three-metal cluster. This observation establishes the preference of the four-metal cluster for Zn^{2+} over Cu^+. When the protein was induced in rabbits by the injection of a $^{113}CdCl_2$ solution, native ^{113}Cd,Zn-MT was extracted from the liver, and an analysis of its ^{113}Cd-NMR spectrum revealed that Zn^{2+} was predominantly bound (>85%) to the three-metal cluster (*25*). ^{113}Cd-NMR analysis of the metal distribution in these three metal–hybrid MTs therefore demonstrated that the two metal clusters display opposite binding affinities. For the four-metal cluster, the preference is Cd > Zn > Cu, and for the three-metal cluster, Cu > Zn > Cd.

The reverse selectivity of the two mammalian metal clusters may be partly rationalized in terms of geometric considerations. Although Cd^{2+} and Zn^{2+} both prefer tetrahedral coordination with sulfur ligands, it is interesting to note that the Zn–S bond length (2.34 Å) is shorter than the Cd–S bond length (2.52 Å) as a result of the smaller ionic radius of Zn^{2+} (0.69 Å) relative to Cd^{2+} (1.03 Å) (*41*). Cd^{2+} binding to the four-metal cluster may be favored over Zn^{2+} because binding of the latter would result in a reduction of the volume of the four-metal cluster leading to increased steric hindrance between the residues in this more complex structural unit. As a comparison, it has been calculated that the volume of the idealized Cd_4 tetrahedron is ~30% larger than the corresponding Zn_4 tetrahedron in the $[M_4(SC_6H_5)_{10}]^{2-}$ compounds which form adamantane-like structures and are therefore closely related to the proposed four-metal cluster of MT (*42*). Cu^+ is known to adopt trigonal coordination with sulfur and therefore its mode of binding may differ from that of Cd^{2+} or Zn^{2+} (*41*). The cysteine positions in the three-metal cluster may be more favorably disposed to trigonal (or other) coordination than those associated with the four-metal cluster. This is consistent with the different binding stoichiometries and chromatographic properties which have been reported for Cu-MT relative to Cd,Zn-MTs (*43,44*). It is, however, possible that the Cu^+ coordination in MT is tetrahedral, as reported from an EXAFS study of the related yeast Cu-MT (*45*).

In the case of homogeneous rabbit ^{113}Cd-MT, the metal ions are more strongly bound to the four-metal cluster. Evidence for this preference is the selective release of Cd^{2+} from the three-metal cluster during isolation (*32*), or titration with ethylenediaminetetraacetate ion (EDTA), as seen by ^{113}Cd-NMR (Y. Boulanger and I. M. Armitage, unpublished observations). The simultaneous disappearance of the $^{113}Cd^{2+}$ ions from this cluster during EDTA titration is also indicative of cooperative dissociation. Although metal exchange without protein aggregation is readily accomplished in the tissue homogenate during isolation by addition of the appropriate metal salts (*32*), exchange in an aqueous solution of the isolated protein in our hands, even under reducing conditions, is not trivial. In an effort to further characterize the mechanism of exchange, experiments are underway to determine the appropriate combination(s) of pH, ionic strength, reducing agents and counter ions which will mimic the conditions in the homogenate.

Two Clusters, Two Domains

Preliminary evidence for the independence of the two mammalian metal clusters is that there is no observable effect on the ^{113}Cd resonances of the four-metal cluster when the three-metal cluster is depleted of Cd^{2+} by EDTA (Y. Boulanger and I. M. Armitage, unpublished observations). Even more striking is the analysis of the ^{113}Cd-NMR spectrum of a polypeptide fragment, designated α_I, which was obtained by proteolytic cleavage of rat liver MT-1 by subtilisin (*46*). This fragment's amino acid composition corresponded to the carboxyl-terminal portion of the metallothionein chain (residues 30–61). It can be seen in Figure 5 that there is an almost direct correspondence between the chemical shifts of the four ^{113}Cd resonances of the α_I-fragment and those attributed to

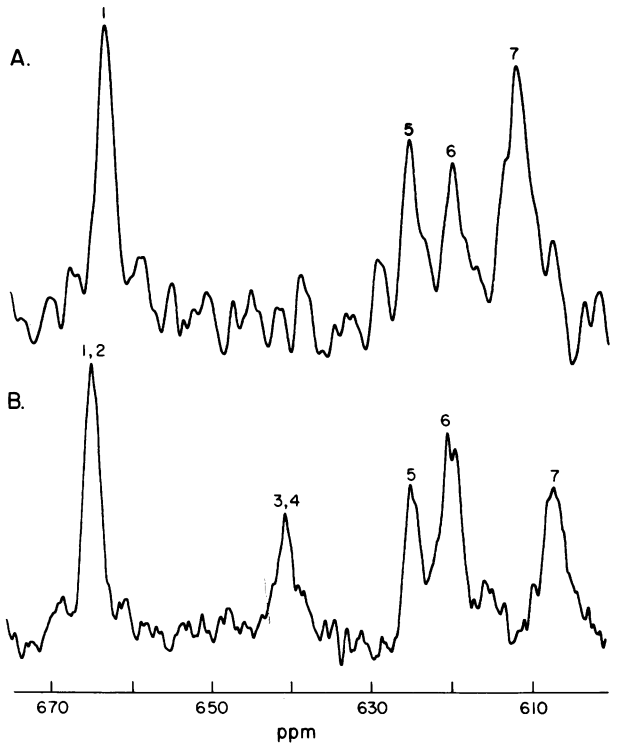

FIGURE 5. Proton-decoupled ^{113}Cd-NMR spectra (44.4 MHz): (A) Cd-α_1-MT fragment from subtilisin digestion of rat liver MT-1 (4.2 mM); (*B*) ^{113}Cd reconstituted liver MT-2 (7.1 mM). The acquisition parameters were: temperature 10°C; spectral width, 10 kHz; pulse angle, 2.5 μsec (40°); recycle tiime, 0.7 sec; and number of transients 15,000 (MT-2) and 220,000 (α_I-MT) (33).

the four-metal cluster of intact human MT-2 (*33*) This provided the first unequivocal evidence for the existence of two separate domains in the structure of metallothionein.

Gene Structure and Evolution

A recent hypothesis states that exons of eukaryotic genes code for the structural and functional domains of proteins (*47*). While in many cases this holds true (*47*), there are certain instances where this proposal falls short (*48,49*). For several proteins, introns in the genetic sequence map for proteolysis cleavage points on the surface of the protein (*49*).

With this in mind, it is interesting to examine the primary structure of the mouse MT-1 (*50,51*) and human MT-2 (*40*) genes. Both these mammalian MT genes have two introns which divide the chain into three exons corresponding to amino acid residues 1–9, 10–31 and 32–61, respectively. The three exons code for 2, 7 and 11 cysteines, respectively. Although our studies are not consistent with the 20 cysteines being distributed over three separate domains, it is apparent that exon 3 codes for the domain containing the four-metal cluster. It is also interesting to note that the cleavage point for subtilisin is two residues removed from the intron 2/exon 3 junction which is consistent with the views of Fletterick et al. (*49*) on the dispositions of proteolysis sites.

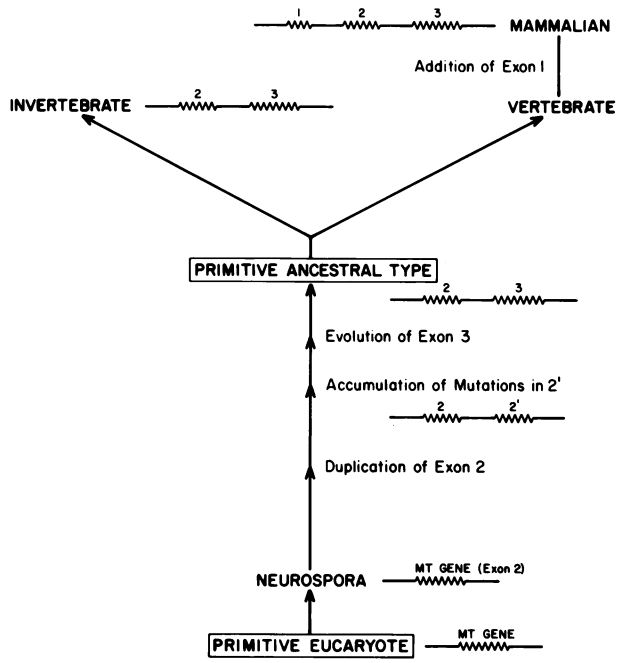

FIGURE 6. Speculation on the phylogeny of the metallothionein gene.

In view of the proposal that duplication, modification and shuffling of exons are mechanisms of evolution (*49*), it seems reasonable to speculate on the development of the MT genes (see Fig. 6). For instance, the MT gene of the mold, *Neurospora crassa,* codes for a protein containing seven cysteines, suggesting that the primordial gene for metallothionein could have been a single exon, similar to exon 2. Perhaps, because of selective pressure to handle a greater volume of essential and nonessential metal ions, this exon was duplicated and with an accumulation of mutations, there evolved a primitive ancestral type gene that contained two exons. Through further evolution, this ancestral gene diverged on the one hand to an invertebrate form which contains 18 cysteines and on the other hand to a vertebrate from which contains 20 cysteines. It is tempting to speculate that the polypeptide sequence of the invertebrate MT with its two three-metal domains corresponds to the polypeptide coded for by exons 2 and 3 of the mammalian gene. Further speculation, how-

ever, must await the sequencing of an invertebrate MT gene. At present, our data on the invertebrate do not reflect any differences in the metal affinities of the two three-metal clusters. It is only with the addition of two more cysteines, which enables the binding of a fourth metal ion, that the metal clusters exhibit different metal affinities. It is therefore plausible to speculate that the evolution of two polynuclear clusters with different physicochemical properties occurred in order to confer on higher organisms a more sophisticated mechanism for metal homeostasis and/or detoxification.

^{1}H-NMR Studies

Substantial data on the three–dimensional structure of metallothioneins have been obtained from the ^{1}H-NMR studies of metallothioneins from different sources (calf, human, rat, rabbit, crab and *Neurospora crassa*) (*34*, S. W. Fesik and I. M. Armitage, unpublished observations). For example, the downfield region (6.5–9.5 ppm) of the ^{1}H-NMR spectra of intact ^{113}Cd-reconstituted rabbit MT and of the rat α_{II}-fragment in 95% H_20 shows 11–13 and 6 well-resolved ^{1}H resonances, respectively (*34*). These resonances are due to slowly exchanging amide protons. The number of resonances is consistent with the results of the Chou-Fasman calculation (*52*) which predict 11 and 6 β-bends for the intact MT and the fragment, respectively. Each β-bend is formed by hydrogen bonding of the NH group of residue *n* to the CO group of residue (*n* + 3), thus forming a hairpin turn. Additional three-dimensional structural data has been obtained by ^{1}H–^{1}H nuclear Overhauser enhancement (NOE) difference spectra which enables the spatial proximity of several residues to be established (*34*).

The complete assignment of the ^{1}H-NMR resonances of metallothionein is not possible solely on the basis of one-dimensional NMR data even at 500 MHz. Several assignments have therefore been made by using two-dimensional NMR techniques [2D J-resolved (*53*), spin-echo correlated spectroscopy (*54*) and 2D correlated spectroscopy (COSY) (*55,56,*)] (S. W. Fesik and I. M. Armitage, unpublished observations). Figure 7 shows an excellent example of the application of one such 2D technique to the elucidation of the ^{1}H-NMR spectrum of crab MT-1. The upper part of the figure shows the one-dimensional spectrum in-which most of the resonances cannot be assigned due to the large number of repetitive residues and overlapping resonances. The lower portion of Figure 7 shows a contour plot of a 2D COSY experiment (*55,56*) in which a number of unequivocal assignments are indicated. The cross peaks in the contour plot correspond to the frequencies of the protons that are scalar coupled. For example, the scalar connectivities between the methyl protons and the α-CH (Ala) and β-CH (Val, Thr) protons are illustrated by a dashed line in the figure connecting the cross peak to the two coupled proton frequencies located on the diagonal. The Val resonances were assigned from their characteristic chemical shifts and the fact that both methyl resonances are scalar coupled to the same β-CH proton. The Thr CH_3 protons are spin-coupled to a β-CH which is scalar connected to an α-CH proton; whereas, the Ala CH_3 is spin-coupled directly to an α-proton. On this basis, the Thr and Ala proton resonances were distinguished. The region of the contour plot within the solid line displays an area of off-diagonal peaks correspond-

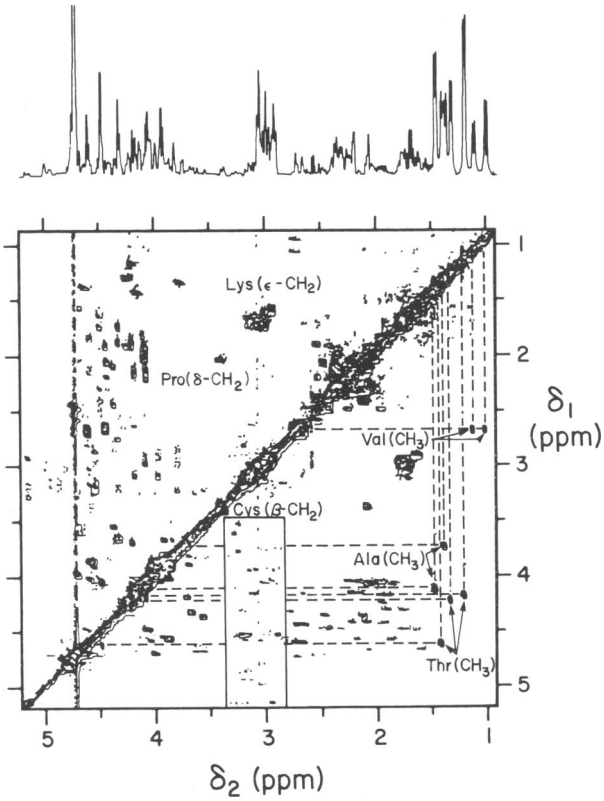

FIGURE 7. Contour plot of a two-dimensional correlated ^{1}H-NMR spectrum of crab ^{113}Cd-MT-1 (10mM) in ^2H_2O obtained at 500 MHz. A (90-t_1-90-acquire)$_n$ pulse sequence was used in which the value of t_1 was incremented by 300 μsec, and 64 scans were acquired for each t_1. The data set consisted of 512 free induction decays (FID), each containing 2K data points. To process the data, the FIDs were zero-filled, multiplied by a sine-bell window function, and Fourier-transformed.

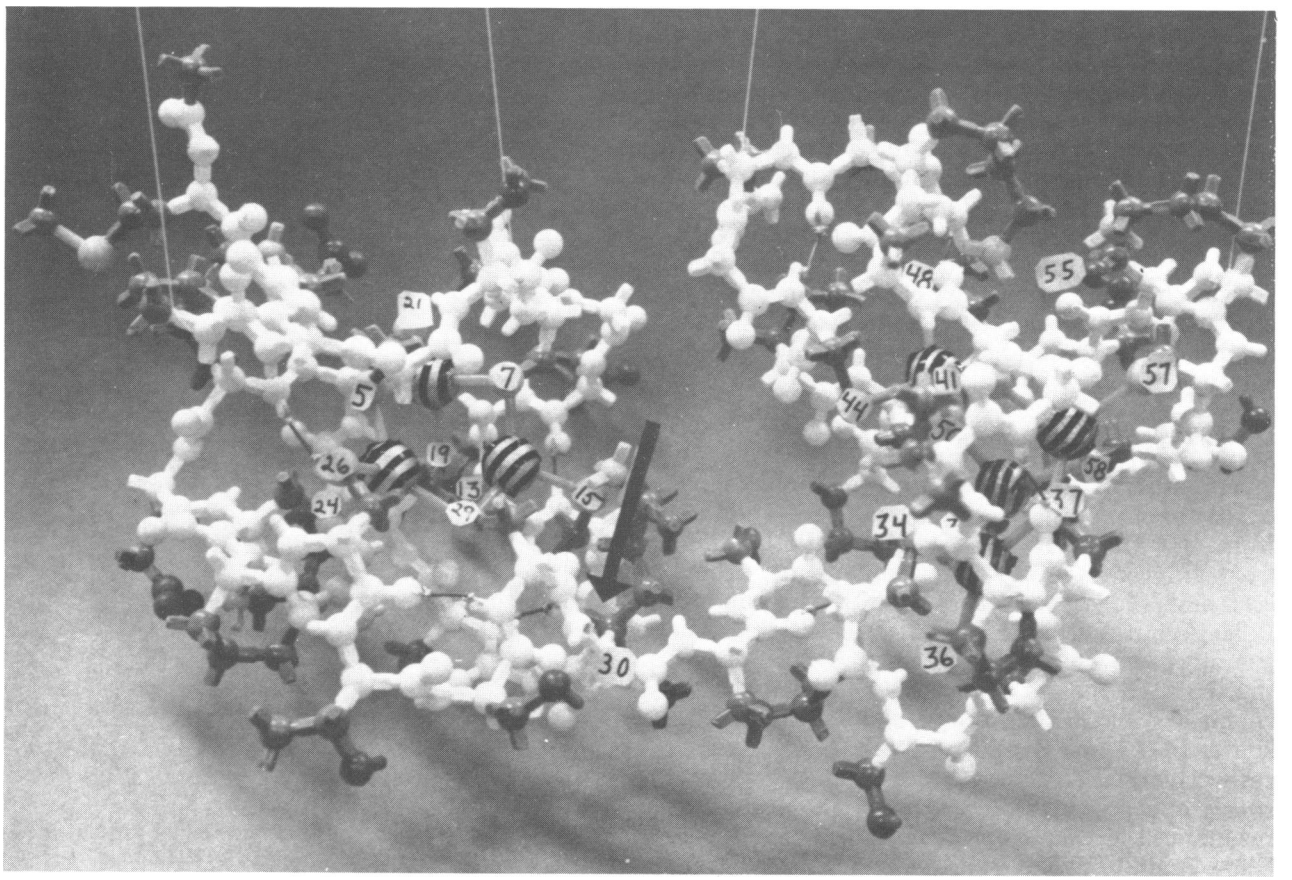

FIGURE 8. Photograph of our proposed three-dimensional model for mammalian MT. The numbers correspond to the residue numbers in the primary structure, and the arrow indicates the subtilisin cleavage point.

ing to the β-CH_2 protons of the 18 Cys residues spin-coupled to their corresponding α-CH protons. By spreading the data into two dimensions, the Lys resonances in this region appear above the diagonal and the different Cys cross peaks are easily resolvable, allowing all of the α-CH Cys protons to be identified. The analysis of the data from the application of these different techniques to MTs from different sources and of different structures is in progress and should allow the assignment of the vast majority of the ^1H resonances. These assignments will then be used for further conformational analysis.

Model for Mammalian Metallothionein

Based on the structural and physicochemical data available, a molecular model of mammalian metallothionein has been constructed and is shown in Figure 8 (*34*). The protein is constructed with two domains, one containing the three- and the other the four-metal cluster, corresponding to the amino-terminal and carboxyl-terminal portions of the protein, respectively. The metal clusters consist of tetrahedral metal centers bound and bridged by cysteine sulfurs, as evidenced by ^{113}Cd-NMR. The 11 β-bends predicted by the Chou-Fasman calculations are also included in this model (*52*).

Whereas it is not possible at this time to determine a unique distribution of the cysteine residues among the individual metal binding sites, the results from the NMR studies of the proteolytically cleaved α_{II}-fragment allowed us to divide the chain into two domains containing: the three-metal cluster (residues 1–29) and the four-metal cluster (residues 30–61). The domain of the three-metal cluster contains four Cys-X-Cys groups (specifically residues 5–7; 13–15; 19–21 and 24–26) and one isolated cysteine (residue 29) (see Fig. 1). In deploying these cysteine residues in the cluster, we have assumed that each Cys-X-Cys group binds to the same metal, because of the

short distance between the cysteines. The five β-bends predicted by the Chou-Fasman program for this region can also be easily built into the model. The domain of the four-metal cluster contains three cysteine groupings: a Cys-Cys-X-Cys-Cys group in positions 33–37, a Cys-X-Cys-Cys group in positions 57–60 and four cysteines in positions 41–50. In the proposed structure of the four-metal cluster we have assumed that adjacent cysteines bind the same metal. Therefore, the cysteine residues in positions 33–37 and 41–50 are ligands of Cd_1 and Cd_5, respectively, and the cysteine residues in positions 57–60 are ligands of Cd_6 and Cd_7. The cysteines at residues 33, 37, 41 and 50 are bridging ligands and are therefore further linked to a second metal ion. The six β-bends, which were predicted for this domain by the Chou-Fasman calculation, are readily incorporated into our model. It is interesting to note that in this model the polypeptide chain is wrapped more tightly around the four-metal cluster. Further tertiary structure is provided by electrostatic interactions and hydrogen bonding involving the side chains of various residues (Ser, Thr) with, for example, the amide carboxyl of the peptide chain (O–H . . . O=C) (*57*). Some of these interactions have been built into our model (*34*).

Conclusion

^{113}Cd–NMR studies have provided detailed information on the structural and spacial relationship of the individual metal sites in MTs. Especially significant are the findings that crab MT shares with mammalian MTs the property of binding its metals in two separate metal-thiolate clusters, but differs in that both are type-B, three-metal clusters, rather than a type B, three- and a type A, four-metal cluster. Despite the evolutionary distance between the invertebrate (crab) and the vertebrates, a high degree of sequence homology exists between MTs from these sources (*35*). In this light, it is possible that the type A, four-metal cluster is a relatively recent evolutionary development occurring sometime after the divergence of invertebrates and mammals from their primordial ancestor. The selective pressure for this is unclear because of the uncertainty which still exists regarding the physiological function of the protein. However, the results of the ^{113}Cd-NMR experiments have demonstrated the opposite selectivity of the two mammalian metal clusters for various metal ions. This would enable the four-metal cluster to sequester the toxic metal ion, Cd^{2+}, while leaving the three-metal cluster available for the regulation and/or metabolism of Zn^{2+} and Cu^{+}. In other words, this development might have occurred in order to impart to vertebrates the ability to handle both essential and nonessential metals with selectivity.

^1H-NMR studies have extended our knowledge of the tertiary structure of the protein and will certainly contribute more substantially in the future. Our present model for the three-dimensional solution structure of mammalian metallothionein is consistent with all the physicochemical data presently available. It should be noted, however, that this is not a unique solution. That is, a final refinement of our model will be necessary when the X-ray crystal structure, currently in progress in the laboratory of C. D. Stout, becomes available. Nevertheless, we are confident that the crystal structure will confirm many of the features of our model and we are continuing in our efforts to elucidate the biological function(s) of this protein.

The financial assistance of National Institutes of Health Grant AM 18778, National Science Foundation grant CHE-7916210, and a North Atlantic Treaty Organization Postdoctoral Fellowship (Y.B.) is gratefully acknowledged.

REFERENCES

1. Nordberg, M., and Kojima, Y. Report from the First International Meeting on metallothionein and other low molecular weight metal-binding proteins. In: Metallothionein (J. H. R. Kägi and M. Nordberg, Eds.), Birkhäuser, Basel, 1979, pp. 41–116.
2. Kojima, Y., and Kägi, J. H. R. Metallothionein. Trends Biochem. Sci. 3: 90–93 (1978).
3. Prinz, R., and Weser, U. A naturally occurring Cu-thionein in *Saccharomyces cerevisiae*. Hoppe-Seyler's Z. Physiol. Chem. 356: 767–776 (1975).
4. Lerch, K. Copper metallothionein, a copper-binding protein from *Neurospora crassa*. Nature 284: 368–370 (1980).
5. Kägi, J. H. R., and Vallee, B. L. Metallothionein: a cadmium and zinc-containing protein from equine renal cortex. J. Biol. Chem. 236: 2435–2442 (1961).
6. Vallee, B. L. Metallothionein: Historical review and perspectives. In: Metallothionein, (J. H. R. Kägi and M. Nordberg, Eds.), Birkhäuser, Basel, 1979, pp. 19–40.
7. Chang, C. C., Lauwerys, R., Bernard, A., Roels, H., Buchet, J. P., and Garvey, J. S. Metallothionein in cadmium-exposed workers. Environ. Res. 23: 422–428 (1980).
8. Squibb, K. S., Cousins, R. J., and Feldman, S. L. Control of zinc-thionein synthesis in rat liver. Biochem. J. 164: 223–228 (1977).
9. Winge, D. R., Premakumar, R., and Rajagopalan, K. V. Metal-induced formation of metallothionein in rat liver. Arch. Biochem. Biophys. 170: 242–252 (1975).
10. Cherian, M. G., and Goyer, R. A. Minireview: metallothioneins and their role in the metabolism and toxicity of metals. Life Sci. 23: 1–10 (1978).
11. Johnson, D. R., and Foulkes, E. C. On the proposed role of metallothionein in the transport of cadmium. Environ. Res. 21: 360–365 (1980).
12. Margoshes, M., and Vallee, B. L. A cadmium protein from equine kidney cortex. J. Am. Chem. Soc. 79: 4813–4814 (1957).

13. Kojima, Y., Berger, C., Vallee, B. L., and Kägi, J. H. R. Amino acid sequence of equine renal metallothionein-1B. Proc. Natl. Acad. Sci. (U.S.) 73: 3413–3417 (1976).
14. Kojima, Y., Berger, C., and Kägi, J. H. R. The amino acid sequence of equine metallothioneins. In: Metallothionein (J. H. R. Kägi and M. Nordberg, Eds.), Birkhäuser, Basel, 1979, pp. 153–161.
15. Huang, I. -Y., Yoshida, A., Tsunoo, H., and Nakajima, H. Mouse liver metallothioneins: complete amino acid sequence of metallothionein-I. J. Biol. Chem. 252: 8217–8221 (1977).
16. Huang, I. -Y., Kimura, M., Hata, A., Tsunoo, H., and Yoshida, A. Complete amino acid sequence of mouse liver metallothionein-II. J. Biochem. 89: 1839–1845 (1981).
17. Kimura, M., Otaki, N., and Imano, M. Rabbit liver metallothionein. Tentative amino acid sequence of metallothionein. In: Metallothionein (J. H. R. Kägi and M. Nordberg, Eds.), Birkhäuser, Basel, 1979, pp. 163–168.
18. Kissling, M. M., and Kägi, J. H. R. Amino acid sequence of human hepatic metallothioneins. In: Metallothionein (J. H. R. Kägi and M. Nordberg, Eds.), Birkhäuser, Basel, 1979, pp. 145–151.
19. Kissling, M. M., and Kägi, J. H. R. Primary structure of human hepatic metallothionein. FEBS Letters 82: 247–250 (1977).
20. Rupp, H., and Weser, U. Circular dichroism of metallothioneins. A structural approach. Biochim. Biophys. Acta 533: 209–226 (1978).
21. Bühler, R. H. O., and Kägi, J. H. R. Spectroscopic properties of zinc-metallothionein. In: Metallothionein (J. H. R. Kägi and M. Nordberg, Eds.), Birkhäuser, Basel 1979, pp. 211–220.
22. Law, A. Y. C., and Stillman, M. J. The effect of pH on Cd^{2+} binding to rat liver metallothionein. Biochem. Biophys. Res. Commun. 94: 138–143 (1980).
23. Vašák, M., Kägi, J. H. R., and Hill, H. A. O. Zinc (II), cadmium (II), and mercury (II) thiolate transitions in metallothionein. Biochemistry 20: 2852–2856 (1981).
24. Rupp, H., and Weser, U. Conversion of metallothionein into Cu-thionein, the possible low molecular weight form of neonatal hepatic mitochrondrocuprein. FEBS Letters 44: 293–297 (1974).
25. Armitage, I. M., and Otvos, J. D. Principles and applications of ^{113}Cd NMR to biological systems. In: Biological Magnetic Resonance, Vol. 4 (L. R. Berliner and J. Reuben, Eds.), Plenum Press, 1982, pp. 79–144.
26. Otvos, J. D., and Armitage, I. M. ^{113}Cd NMR of metallothionein: direct evidence for the existence of polynuclear metal binding sites. J. Am. Chem. Soc. 101: 7734–7736 (1979).
27. Otvos, J. D., and Armitage, I. M. Structure of the metal clusters in rabbit liver metallothionein. Proc. Natl. Acad. Sci. (U.S.) 77: 7094–7098 (1980).
28. Boulanger, Y., and Armitage, I. M. ^{113}Cd NMR study of the metal cluster structure of human liver metallothionein. J. Inorg. Biochem. 17: 147–153 (1982).
29. Briggs, R. W., and Armitage, I. M. Evidence for site-selective metal binding in calf liver metallothionein. J. Biol. Chem. 257: 1259–1262 (1982).
30. Armitage, I. M., Otvos, J. D., Briggs, R. W., and Boulanger, Y. Structure elucidation of the metal-binding sites in metallothionein by ^{113}Cd NMR. Fed. Proc. 41: 2974–2980 (1982).
31. Otvos, J. D., Olafson, R. W., and Armitage, I. M. Structure of an invertebrate metallothionein from *Scylla serrata*. J. Biol. Chem. 257: 2427–2431 (1982).
32. Otvos, J. D., and Armitage, I. M. Elucidation of metallothionein structure by ^{113}Cd NMR. In: Biochemical Structure Determination by NMR (B. D. Sykes, J. Glickson, and A. A. Bothner-By, Eds.), Marcel Dekker, New York, 1981, pp. 65–96.
33. Boulanger, Y., Armitage, I. M., Miklossy, K.-A., and Winge, D. R. ^{113}Cd NMR study of a metallothionein fragment. J. Biol. Chem. 257: 13717–13719 (1982).
34. Boulanger, Y., Goodman, C. M., Forte, C. P., Fesik, S. W., and Armitage, I. M. Model for mammalian metallothionein structure. Proc. Natl. Acad. Sci. (U.S.) 80: 1501–1505 (1983).
35. Lerch, K., Ammer, D., and Olafson, R. W. Crab metallothionein: primary structure of metallothioneins 1 and 2. J. Biol. Chem. 257: 2420–2426 (1982).
36. Olafson, R. W., Kearns, A., and Sim, R. G. Heavy metal induction of metallothionein synthesis in the hepatopancreas of the crab *Scylla serrata*. Comp. Biochem. Physiol. 62B: 417–424 (1979).
37. Olafson, R. W., Sim, R. G., and Boto, K. G. Isolation and chemical characterization of the heavy metal-binding protein metallothionein from marine invertebrates. Comp. Biochem. Physiol. 62B: 407–416 (1979).
38. Murphy, P. DuBois, Stevens, W. C., Cheung, T. T. P., Lacelle, S., Gerstein, B. C., and Kurtz, D. M., Jr. High-resolution ^{113}Cd NMR of solids. Correlation of spectra with the molecular structure of a decanuclear cadmium (II) complex. J. Am. Chem. Soc. 103: 4400–4405 (1981).
39. Haberkorn, R. A., Que, L., Jr., Gillum, W. O., Holm, R. H., Liu, C. S., and Lord, R. C. Cadmium-113 Fourier transform nuclear magnetic resonance and Raman spectroscopic studies of cadmium (II)-sulfur complexes, including $[Cd_{10}(SCH_2CH_2OH)_{16}]^{4+}$. Inorg. Chem. 15: 2408 (1976).
40. Karin, M., and Richards, R. I. Human metallothionein genes—primary structure of the metallothionein-II gene and a related processed gene. Nature (London) 299: 797–802 (1982).
41. Tossell, J. A., and Vaughan, D. J. Relationships between valence orbital bonding energies and crystal structures in compounds of copper, silver, gold, zinc, cadmium and mercury. Inorg. Chem. 20: 3333–3340 (1981).
42. Hagen, K. S., Stephan, D. W., and Holm, R. H. Metal ion exchange reactions in cage molecules: the systems $[M_{4-n}M'_n(SC_6H_5)_{10}]^{2-}$ [M, M′ = Fe(II), Co(II), Zn(II), Cd(II)] with adamantane-like stereochemistry and the structure of $[Fe_4(SC_6H_5)_{10}]^{2-}$. Inorg. Chem. 21: 3928–3936 (1982).
43. Suzuki, K. T., and Maitani, T. Metal-dependent properties of metallothionein: replacement *in vitro* of zinc in zinc-thionein with copper. Biochem. J. 199: 289–295 (1981).
44. Winge, D. R., Geller, B. L., and Garvey, J. Isolation of copper thionein from rat liver. Arch. Biochem. Biophys. 208: 160–166 (1981).
45. Bordas, J., Koch, M. H. J., Hartmann, H.-J., and Weser, U. Tetrahedral copper-sulphur coordination in yeast Cu-thionein. FEBS. Letters 140: 19–21 (1982).
46. Winge, D. R. and Miklossy, K.-A. Domain nature of metallothionein. J. Biol. Chem. 257; 3471–3476 (1982).
47. Gilbert, W. Why genes in pieces? Nature 271: 501 (1978).
48. Craik, C. S., Rutter, W. J., and Fletterick, R. Splice junctions: association with variation in protein structure. Science 220: 1125–1129 (1983).
49. Craik, C. S., Sprang, S., Fletterick, R., and Rutter, W. J. Intron-exon splice junctions map at protein surfaces. Nature (London) 299: 180–182 (1982).
50. Durnam, D. M., Perrin, F., Gannon, F., and Palmiter, R. D. Isolation and characterization of the mouse metallothionein-I gene. Proc. Natl. Acad. Sci. (U.S.) 77: 6511–6515 (1980).
51. Glanville, N., Durnam, D. M., and Palmiter, R. D. Struc-

ture of mouse metallothionein-I gene and its mRNA. Nature 292: 267–269 (1981).
52. Fasman, G. D. Prediction of protein conformation from the primary structure. Ann. N.Y. Acad., 348: 147–159 (1980).
53. Aue, W. P., Karhan, J., and Ernst, R. R. Homonuclear broad band decoupling and two-dimensional J-resolved NMR spectroscopy. J. Chem. Phys. 64: 4226–4227 (1976).
54. Nagayama, K., Wüthrich, K., and Ernst, R. R. Two-dimensional spin echo correlated spectroscopy (SECSY) for ^{1}H NMR studies of biological macromolecules. Biochem. Phys. Res. Commun. 90: 305–311 (1979).
55. Aue, W. P., Bartholdi, E., and Ernst, R. R. Two-dimensional spectroscopy. Application to NMR. J. Chem. Phys. 64: 2229–2246 (1976).
56. Wagner, G., Kumar, A., and Wüthrich, K. Systematic application of two-dimensional ^{1}H NMR techniques for studies of proteins. Eur. J. Biochem. 114: 375–384 (1981).
57. Vašák, M., Galdes, A., Hill, H. A. O., Kägi, J. H. R., Bremner, I., and Young, B. W. Investigation of the structure of metallothioneins by proton nuclear magnetic resonance spectroscopy. Biochemistry 19: 416–425 (1980).